Acta Polytechnica **53**(SUPPLEMENT):534-537, 2013 doi:10.14311/AP.2013.53.0534

© Czech Technical University in Prague, 2013 available online at http://ojs.cvut.cz/ojs/index.php/ap

# THE $^2$ H( $\alpha$ , $\gamma$ ) $^6$ LI REACTION AT LUNA AND BIG BANG NUCLEOSYNTHETIS

### Carlo Gustavino\*

INFN Sezione di Roma, I-00185 Roma, Italy

\* corresponding author: carlo.gustavino@roma1.infn.it

ABSTRACT. The  ${}^2H(\alpha, \gamma){}^6Li$  reaction is the leading process for the production of  ${}^6Li$  in standard Big Bang Nucleosynthesis. Recent observations of lithium abundance in metal-poor halo stars suggest that there might be a  ${}^6Li$  plateau, similar to the well-known Spite plateau of  ${}^7Li$ . This calls for a re-investigation of the standard production channel for  ${}^6Li$ . As the  ${}^2H(\alpha, \gamma){}^6Li$  cross section drops steeply at low energy, it has never before been studied directly at Big Bang energies. For the first time the reaction has been studied directly at Big Bang energies at the LUNA accelerator. The preliminary data and their implications for Big Bang nucleosynthesis and the purported  ${}^6Li$  problem will be shown.

KEYWORDS: LUNA experiment, nuclear astrophysics, Big Bang nucleosynthesis, <sup>6</sup>Li abundance,  $^2H(\alpha, \gamma)^6Li$  reaction.

# 1. Introduction

In its standard picture, Big Bang nucleosynthesis occurs during the first minutes of universe, with the formation of light isotopes such as D,  $^3$ He,  $^4$ He,  $^6$ Li and  $^7$ Li, through the reaction chain shown in Fig. 1. Their abundance depends on the standard model physics, on the baryon-to-photon ratio  $\eta$  and on the nuclear cross sections of involved processes. Cosmic Microwave Background (CMB) experiments provide the  $\eta$  value with high precision (percent level) [1]. Indeed, the BBN theory makes definite predictions for the abundances of the light elements as far as the nuclear cross sections of leading processes are known.

The observed abundances of D,  $^3$ He, and  $^4$ He are in good agreement with calculations, confirming the overall validity of BBN theory. On the other hand, the observed abundance of  $^7$ Li is a factor  $2 \div 3$  lower than the predicted abundance (see Fig. 2). The amount of  $^6$ Li observed in metal poor stars is unexpectedly large compared to Big Bang Nucleosynthesis (BBN) predictions, about 3 order of magnitude higher than the calculated value (see Fig. 2). Even though many of the claimed  $^6$ Li detections may be in error, for a very few metal-poor stars there still seems to be a significant amount of  $^6$ Li [2]. The difference between observed and calculated values may reflect unknown post-primordial processes or physics beyond the Standard Model.

The leading process to synthesize  $^6\text{Li}$  is the  $^2\text{H}(\alpha, \gamma)^6\text{Li}$  reaction. The  $^2\text{H}(\alpha, \gamma)^6\text{Li}$  cross section is very small at BBN energies  $(30 \lesssim E(\text{keV}) \lesssim 400)$ , because of the repulsion between the interacting nuclei. Therefore, it has never been measured experimentally, and theoretical predictions remain uncertain [3]. This process has been experimentally studied only for energies greater than 1 MeV and around the 711 keV [4, 5]. There are two attempts to determine the  $^2\text{H}(\alpha, \gamma)^6\text{Li}$ 

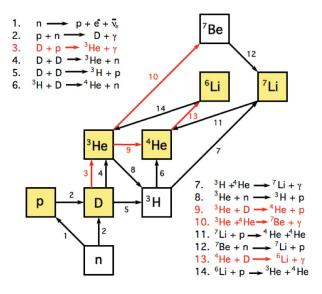


FIGURE 1. Leading processes of Big Bang Nucleosynthesis. The red arrows show the reactions measured by the LUNA collaboration. Yellow boxes marks stable isotopes.

cross section at BBN energies, using the Coulomb dissociation technique [6, 7]. In this approach, an energetic  $^6{\rm Li}$  beam passes close to a target of high nuclear charge. In this way, the time-reversed reaction  $^6{\rm Li}(\gamma,\alpha)^2{\rm H}$  is studied using virtual photons which are exchanged.

The measurements mentioned above are shown in Fig. 3. In the figure, the cross section  $\sigma$  is parameterized with the astrophysical factor S(E), defined by the formula

$$\sigma(E) = \frac{S(E) e^{-2\pi\eta}}{E}.$$
 (1)

S(E) contains all the nuclear effects and, for non-resonant reactions, it is a smoothly varying function

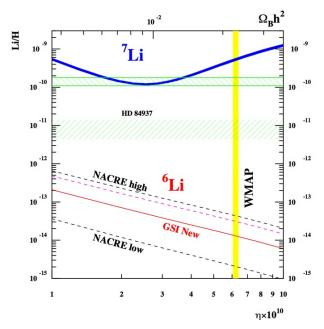


FIGURE 2. Abundances of  $^7\mathrm{Li}$  and  $^6\mathrm{Li}$  as a function of the  $\eta$  parameter. Observations are represented as green, horizontal dashed band. The blue band shows the calculated abundance of  $^7\mathrm{Li}$ . The calculated abundance of  $^6\mathrm{Li}$  is obtained using the NACRE compilation recommended values (dashed lines). The vertical yellow band indicates the  $\eta$  parameter as measured by the WMAP experiment.

of energy. The exponential term takes into account the coulomb barrier. The Sommerfeld parameter  $\eta$  is given by  $2\pi\eta=31.29Z_1Z_2(\mu/E)^{1/2}$ .  $Z_1$  and  $Z_2$  are the nuclear charges of the interacting nuclei.  $\mu$  is their reduced mass (in units of a.m.u.), and E is the center of mass energy (in units of keV).

As Coulomb dissociation measurements strongly depends on the theoretical assumptions because nuclear effects are dominant, only a direct measurement of  $^{2}$ H( $\alpha$ ,  $\gamma$ ) $^{6}$ Li reaction in the BBN energy range can give a reliable base to compute the <sup>6</sup>Li primordial abundance. The present papers reports on the first direct measurement of the  $^6\text{Li}(\gamma, \alpha)^2\text{H}$  performed by the LUNA collaboration (LUNA – Laboratory for Underground Nuclear Astrophysics). The measurement has been performed with the unique underground accelerator in the world, situated at the LNGS laboratory (LNGS – Laboratorio Nazionale del Gran Sasso). The "Gran Sasso" mountain provides a natural shielding which reduces the muon and neutron fluxes by a factor  $10^6$  and  $10^3$ , respectively. The suppression of the cosmic ray induced background also allows an effective suppression of the  $\gamma$ -ray activity by a factor  $10^2 \div 10^5$ , depending on the photon energy [8].

#### 2. Experimental set-up

Figure 5 shows the experimental set-up used for the  $^2H(\alpha,\,\gamma)^6Li$  reaction. The measurement is based on the use of the 400 kV accelerator, which provides an  $\alpha$  beam of high intensity. The  $\alpha$  beam impinges a

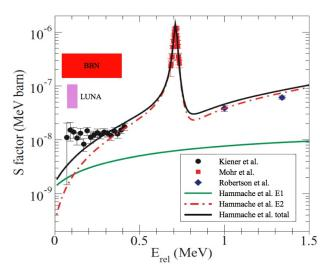


FIGURE 3. The astrophysical factor of the  ${}^2H(\alpha, \gamma){}^6Li$  reaction as a function of the center-of-mass energy. Direct [4, 5] and indirect measurements [6, 7] are reported. The BBN energy region and the energy range studied by LUNA are also reported.

windowless gas target of  $D_2$ , with a typical operating pressure of 0.3 mbar. The signal is maximized by stretching the beam intensity up to about 350  $\mu$ A and by using a geometry with the germanium detector close to the beam line (2 cm apart), to increase its acceptance. The intrinsic low level of natural background of LNGS is further reduced by means of a  $4\pi$  lead shield around the reaction chamber and the Ge detector. Everything is enclosed in a radon box flushed with high purity  $N_2$ , to reduce and stabilize the  $\gamma$  activity due to the radon decay chain.

The measurement of the  $^2\text{H}(\alpha, \gamma)^6\text{Li}$  reaction is affected by an inevitable beam induced background. In fact, the  $^2\text{H}(\alpha, \alpha)^2\text{H}$  Rutherford scattering induces a small number of  $^2\text{H}(^2\text{H}, n)^3\text{H}$  and  $^2\text{H}(^2\text{H}, p)^3\text{H}$  reactions. While the  $^2\text{H}(^2\text{H}, p)^3\text{H}$  reaction is not a problem in this context, the neutrons produced by the  $^2\text{H}(^2\text{H}, n)^3\text{He}$  reaction ( $E_{n(cm)} = 2450\,\text{keV}$ ) induce (n,n' $\gamma$ ) reactions in the Ge detector and in the surrounding materials (lead, steel, copper), generating a beam-induced background in the  $\gamma$ -ray spectrum, in particular around 1.6 MeV, where the capture transition to the ground state of  $^6\text{Li}$  is expected. To reduce the neutron production, a tube 16 cm long, with a square cross section of  $2 \times 2\,\text{cm}^2$  is inserted inside the chamber.

The tube strongly reduces the effective path for the scattered deuterons and therefore the neutron yield due to the  $^2\mathrm{H}(^2\mathrm{H,~n})^3\mathrm{He}$  reaction is reduced at the level of few neutrons/second. Finally, one silicon detector is faced to the gas target volume to monitor the running conditions through the detection of protons generated in the  $^2\mathrm{H}(^2\mathrm{H,~p})^3\mathrm{H}$  reaction ( $E_{\mathrm{p(cm)}}=3022\,\mathrm{keV}$ ). The measurement of the number of protons detected is strictly related to the number of neutrons produced, since the cross sections of the two

Carlo Gustavino Acta Polytechnica

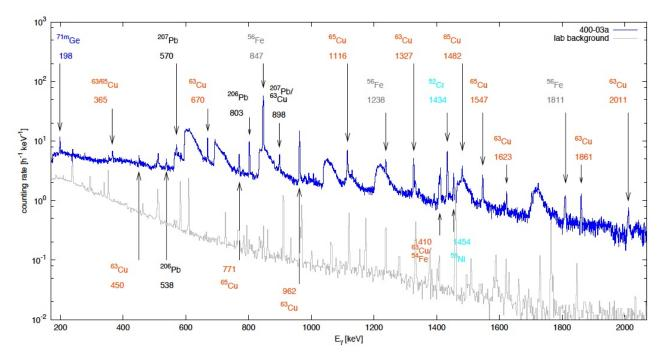


FIGURE 4. Spectra taken with the Ge detector. Blue full line: Beam induced background spectrum at  $E_{\alpha} = 400 \text{ keV}$  and  $P_{\text{target}} = 0.3 \text{ mbar}$ . Grey thin line: laboratory background.

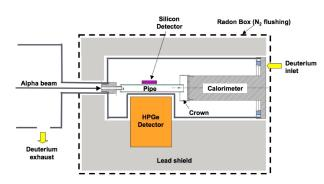


FIGURE 5. Experimental setup.

conjugate  ${}^2\mathrm{H}({}^2\mathrm{H},\,\mathrm{n}){}^3\mathrm{He}$  and  ${}^2\mathrm{H}({}^2\mathrm{H},\,\mathrm{p}){}^3\mathrm{H}$  reactions are well known.

Figure 4 shows the Ge spectrum at  $E_{\alpha} = 400 \, \text{keV}$  and  $P_{\text{deuterium}} = 0.3 \, \text{mbar}$ . Various transitions due to the interaction of neutrons with the Germanium and the surrounding materials can be identified.

# 3. Method

The Energy of  $\gamma$ 's coming from  $D + \alpha$  reaction strongly depends on the beam energy, through the relationship

$$E_{\gamma} = 1473.8 + E_{\rm CM} \pm \Delta E_{\rm doppler}.$$
 (2)

As shown in Fig. 6, the  $\gamma$ -rays energy strongly depends on the beam energy. The Region of Interest (RoI) is about 30 keV wide, because of the Doppler broadening.

As the  $\gamma$ 's produced the  ${}^2H(\alpha, \gamma){}^6Li$  reaction strongly depends on the beam energy, it is possible to extract the signal with a measurement performed in two steps:

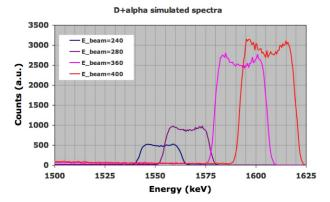
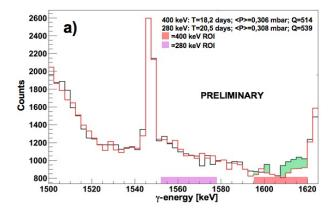


FIGURE 6. Simulated full peak detection of  $\gamma$ 's from  $^2H(\alpha, \gamma)^6Li$  in the LUNA Ge detector, at different beam energy. Note the Doppler broadening of about 30 keV and the dependence with the beam energy.

- (1.) Measurement with  $E_{\rm beam} = 400 \, \rm keV$  on  $D_2$  target. The Ge spectrum is mainly due to the background induced by neutrons. The  $^2{\rm H}(\alpha, \gamma)^6{\rm Li} \ \gamma$  signal is expected in a well defined energy region (1592  $\div$  1620 keV, see Fig. 6).
- (2.) Same as (1.), but with  $E_{\text{beam}} = 280 \text{ keV}$ . The background is essentially the same as before, while the gammas from the  ${}^{2}\text{H}(\alpha, \gamma){}^{6}\text{Li} \ \gamma$  reaction are shifted to  $1555 \div 1578 \text{ keV}$  (see Fig. 6).

Figure 7a shows the spectra with  $E_{\alpha}=400,280\,\mathrm{keV}$ , respectively. A counting excess is clearly visible in the  $E_{\alpha}=400\,\mathrm{keV}$  RoI. Unfortunately, at  $E_{\alpha}=280\,\mathrm{keV}$  the very low reaction yield prevents from any conclusion statistically significant. To verify that the counting excess at  $E_{\alpha}=400\,\mathrm{keV}$  is a genuine  $\gamma$  signal com-



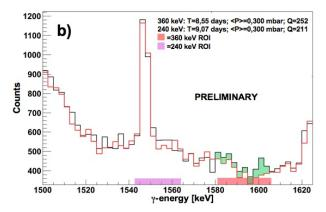


FIGURE 7. a) Experimental Ge spectra for  $E_{\rm beam}=400\,{\rm keV}$  (black line) and for  $E_{\rm beam}=280\,{\rm keV}$  (red line); b) experimental Ge spectra for  $E_{\rm beam}=360\,{\rm keV}$  (black line) and for  $E_{\rm beam}=240\,{\rm keV}$  (red line). T,  $\langle P \rangle$ , Q are respectively the measurement time, the averaged target pressure, the integrated beam current. The bands indicate the RoI at  $E_{\alpha}=400\,{\rm keV}$  RoI and  $E_{\alpha}=280\,{\rm keV}$  a), and the RoI at  $E_{\alpha}=360\,{\rm keV}$  RoI and  $E_{\alpha}=240\,{\rm keV}$  b). Note the counting excess visible in correspondence of the 400 keV RoI. As foreseen, the counting excess shifts to the  $E_{\alpha}=360\,{\rm keV}$  RoI in b).

ing from the  $^2\mathrm{H}(\alpha,\gamma)^6\mathrm{Li}$  reactions, the measurement has been repeated by shifting the beam energies to  $E_{\alpha}=360,240\,\mathrm{keV}$ . As shown in Fig. 7b, the counting excess at the higher energy is shifted as expected, even though the worst signal/noise ratio and the shorter measuremet time.

# 4. Conclusion

The cross section of  ${}^2{\rm H}(\alpha,\,\gamma)^6{\rm Li}$  reaction has been measured for the first time at BBN energy. Although the data analysis is still in progress, the LUNA measurement excludes a nuclear solution for the purported  ${}^6{\rm Li}$  problem. The observation of a "huge" amount of  ${}^6{\rm Li}$  in metal-poor stars must be explained in a different way, e.g. systematics in the  ${}^6{\rm Li}$  observation or physics beyond the Standard Model. In any case, a solid experimental footing is now available to calculate the  ${}^6{\rm Li}$  primordial abundance.

#### References

- [1] D.N. Spergel, et al., 2007, ApJS, 170, 377
- [2] See proceedings of "lithium in the Cosmos", 27-29 february, Paris
- [3] L. Marcucci, K. Nollett, R. Schiavilla, and R. Wiringa, Nucl. Phys. A 777, 111 (2006)
- [4] P. Mohr et al., Phys. Rev. C 50, 1543 (1994)
- [5] R. G. H. Robertson *et al.*, Phys. Rev. Lett. 47, 1867 (1981)
- [6] J. Kiener et al., Phys. Rev. C 44, 2195 (1991)
- [7] F. Hammache et al., Phys. Rev. C 82, 065803 (2010), 1011.6179
- [8] A. Caciolli et al, Eur. Phys. J. A 39, 179–186

#### DISCUSSION

Maurice H.P.M. van Putten — Could the excess of <sup>6</sup>Li in Pop III stars be due to inhomogeneities in primordial Li production due to density fluctuaction? That is <sup>6</sup>Li formation is a binary reaction product with a rate proportional to the density squared, and Pop III stars form selectively out of initially overdense region.

Carlo Gustavino — In my opinion it is difficult to explain the purported <sup>6</sup>Li excess in this way, because the barionic density determines not only the <sup>6</sup>Li abundance but also the amount of all the other primordial isotopes. In particular, deuterium abundance is very sensitive to the barionic density, but observations are in good agreement with calculations.